An experimental investigation of a low Reynolds number turbulent boundary layer subject to an adverse pressure gradient

By J. H. WATMUFF

Summary

This report covers a 12 month period from the beginning of the project. The project concerns an experimental study of a very low Reynolds number turbulent boundary layer subject to an adverse pressure gradient. The work is being performed in the Boundary Layer Wind Tunnel in the Fluid Mechanics Laboratory at NASA Ames Research Center in collaboration with Dr. R.V. Westphal. The aim is to obtain highly accurate mean-flow and turbulence measurements under conditions that can be closely related to the numerical simulations of Philippe Spalart for the purposes of CFD validation. It is expected that the experimental results will also serve as a useful contribution to the research literature in their own right.

Much of the Boundary Layer Wind Tunnel has been completely rebuilt with a new wider contraction and working section which will improve compatibility with the simulations. A unique sophisticated high-speed computer controlled 3D probe traversing mechanism has also been integrated into the new test section. Construction of the tunnel and traverse has consumed a large fraction of the period covered by this report and is discussed in some detail. The hardware is now complete, and measurements are in progress. The mean-flow data indicate that a suitably two-dimensional base flow has been established.

Automation of the probe positioning and data acquisition have led to a decreased running time for total pressure measurements. However, the most significant benefits are expected to occur when using hot-wire probes. Calibrations can be performed automatically and there is no need to handle fragile probes when moving between measuring stations. Techniques are being developed which require sampling of the signals from moving hot-wire probes on the basis of their position in the flow. Measurements can be made in high intensity turbulence by flying probes upstream at high speed so that the relative magnitude of the turbulent velocity fluctuations are reduced. In regions where the turbulence intensity is not too large, the probe can also be repetitively scanned across very dense spatial grids in other directions. With this new technique, a complete profile can be measured in about 1/3 the time and with a spatial density about 50 times that obtainable using a stationary probe.

1. Background

1.1 CFD Simulations

The numerical method used by Spalart (1988) is spectral in space and second-order in time. An important feature of the method is that there is no turbulence modelling. However, this requires a high grid density which restricts the simulations to low Reynolds numbers i.e. $R_\theta < 1500$. Periodic spanwise and streamwise conditions are used and a multiple-scale procedure is applied to approximate slow streamwise growth. The key assumptions are that the streamwise evolution of the flow is slow and that the straining of the turbulence by the mean-flow can be neglected. Spalart has suggested that the assumption of small streamwise growth will cause the method to breakdown for large adverse pressure gradients.

1.2 Relationship between the experiment and simulation

There are three major requirements in the relationship between the experiment and simulation. Firstly, the Reynolds number of the experiment must match that of the simulation precisely. Secondly, the experiment and simulation also must have closely matched initial conditions. The simulation begins at the first station with an equilibrium boundary layer. A mildly favorable pressure gradient can be used to very closely approximate a "self-preserving layer" in the experiment, i.e. by careful experimental design the boundary layer can be maintained at almost constant thickness over some streamwise distance before being subjected to the adverse pressure gradient. Following a suggestion by Inman and Bradshaw (1981) the length of this region could be increased to allow any upstream trip effects to decay before the region of interest. Finally, accurate experimental pressure coefficient (C_p) measurements with high spatial resolution are required as an input for the simulation. A suitable flow configuration for the computations would be one in which the boundary layer experienced a non-dimensional pressure gradient $\beta_x = \frac{\delta^*}{\tau_w}\frac{dP}{dx} \approx 2$ at a maximum $R_\theta \approx 1500$.

1.3 Preliminary experimental measurements

The combined requirements of low Reynolds number and accurate pressure measurements precludes the use of water as a flow medium or the use of very low air velocities (e.g. 0.5 m/s) for the experiment. R.V. Westphal used momentum integral boundary layer calculations as a design tool to show that the Boundary Layer Wind Tunnel in its old form was a suitable facility for the experiment. Preliminary mean-flow measurements verified that this facility could duplicate the Reynolds number and pressure gradient requirements of the simulations. A flat test surface was employed for the boundary layer development, and the pressure gradient was imposed by a contoured upper control wall. The inlet flow velocity was 8.2 m/s. An inlet free-stream velocity around 8 m/s was considered to be close to the lower limit for accurate C_p measurements, i.e. a total head of

0.15 inches of water with an accuracy of ±1%. The mean-flow two-dimensionality appeared to be good since the streamwise momentum balance was found to be within 10%.

In the region of adverse pressure gradient at an $R_\theta \approx 1500$ the reduced profile data showed a $\beta_x \approx 0.7$ which is a little low. A stronger adverse pressure gradient would be required for the current experiment. Also the inlet unit Reynolds number appeared to be a little high. A high inlet unit Reynolds number is undesirable since it shortens the physical distance over which the experiment matches the capabilities of the simulation.

2. New Tunnel Contraction, Test Section and Traverse

2.1 Tunnel Contraction

When formulating the current experiment, it was desirable to use a lower inlet free-stream velocity which would reduce the inlet unit Reynolds number and also provide for better spatial and temporal resolution of hot-wire measurements. However, two factors had to be considered before a lower inlet velocity could be adopted. Firstly, the accuracy of the C_p measurements would need to be maintained. Secondly, an increase in the total free-stream unsteadiness (from about 0.25% to around 0.5%) was observed at low tunnel speeds.

The first restraint was relieved by purchasing the most accurate and sensitive commercially available pressure transducer. This allows the inlet free-stream velocity to be lowered to around 6 m/s (i.e. a total head around 0.08 inches of water) while still maintaining an accuracy of ±1% for the C_p measurements. The second problem appeared to be related to the tunnel fan which was operating near the lower extremity of its characteristics. It was evident that a further drop in the fan speed using the original form of contraction and test section would lead to even more unsteadiness. Instead the flow area of the test section inlet was increased by 50% from 80cm x 20cm to 100cm x 24cm, allowing a lower inlet velocity but at a higher fan speed. This required designing a new 5:1 2D contraction to replace the original 7.5:1 3D version.

Theoretical methods were used for selecting a new Boundary Layer Wind Tunnel contraction design from a number of alternatives. The pressure distribution on the side walls was estimated using a potential flow method. The numerical solution of the stream function inside the contraction and inside upstream and downstream extensions of constant area was used to calculate the velocities on the boundary and the pressure distribution was obtained from the Bernouilli equation. The evolution of the contraction side wall laminar boundary layer subject to this pressure distribution was calculated using a momentum integral method. The effects of streamline curvature and convergence were neglected. The calculations showed that the new contraction design is not likely to cause separation.

2.2 High-speed probe traverse integral with test-section

The numerical simulations usually have very high spatial resolution (e.g. Spalart (1988) used up to 10^7 grid points) but only for a limited number of time steps. This is in complete contrast to the experimental situation where almost unlimited temporal information is available but with very limited spatial content. One way of reducing this discrepancy is for the experimentalist to increase the spatial content of measurements. This dictates that multiple probes and/or more sophisticated traversing equipment be used.

In view of the above considerations, a high-speed 3D computer-controlled probe traversing system has been built. The range of motion is 2.5m in the streamwise X-direction, 0.1m in the Y-direction normal to the wall and 0.5m in the spanwise Z-direction. Minimum top speeds of around 3 m/s in the X-direction and 1.5 m/s in the Y- and Z-directions were desired. These speeds can be reached over a short enough distance with accelerations of 2 g's. Linear stepping motors satisfy the requirements for the Y- and Z-axes for accurate (0.05 mm) high speed (1.5 m/s) positioning. The probe and sting are carried directly by the Y-axis motor. The Y-axis motor rides on a steel platen which is attached to the Z-axis motor, linear bearing and platen assembly. The Z-axis assembly is supported above the test wall within the working section by a gantry which spans the 1m distance between the side walls.

The requirements of the gantry are low mass (to minimize inertial loading), high stiffness (to minimize deflections), and small projected area (to minimize aerodynamic interference). Therefore, the gantry was constructed in the form of a 1m wide truss using sections cut from thin sheets of carbon-fiber composite which were bonded together with epoxy resin. By itself the gantry weighs about 2Kg which is less than 10% of the total movable mass. The total projected area of everything (i.e. the gantry, bearing rails, motors, platens etc.) located within the tunnel is equal to a one inch thick object spanning the tunnel side walls so the blockage is not excessive. Loading the gantry with a 10Kg weight in the center of its one meter span results in a deflection of only 0.05mm. The ends of the gantry are fixed to carriages which move on linear bearings in the X-direction.

The gantry is propelled in the X-direction by a brushless linear d.c. motor which reacts with a long magnet track to provide a maximum propulsive force of 80lbf. The motor is operated as a closed loop servo system with feedback provided by a linear quadrature encoder with a resolution of 10 micron. The maximum speed of the gantry has been tested at 3 m/s. Current linear stepping motor technology cannot match this performance. The two linear bearing rails are fixed to adapter plates which are bolted to a 1.2 x 3.0 m (4 x 10 foot) optics table. One of these adapter plates also supports the magnet track and linear encoder. The optics table provides an extremely rigid mounting platform for the entire assembly. Another significant benefit of the optics table is that it provides

an extremely flat reference surface for alignment purposes.

Measurements are made in the boundary layer forming on a test plate which consists of a 0.375 ± 0.005 inch thick ground aluminum toolplate approximately 1m wide by 2.1m in length. The plate is supported above the optics table by machined standoffs. A dial gauge attached to the traverse indicated that the deviations of the test-plate over the entire traversable X-Z plane were within ± 0.15 mm. The X-axis motor and twin-rail linear bearings are located beneath the test-plate, and rubber strips are attached to the side walls and to the plate to seal the slots that provide access for mounting the gantry. The side walls and flexible ceiling which complete the test-section are attached to a frame that is bolted to the optics table. Full access to the test-plate and traverse assembly can be obtained in minutes by releasing the bolts and hoisting the frame away with a crane.

3. Benefits of the Traverse–Some New Techniques

Automation of the high-speed 3D traverse reduces the time taken for experiments since repetitive control commands do not have to be performed manually. Although this leads to decreased running time for total pressure measurements, the most significant benefits occur when using hot-wire probes.

Hot-wire probes can only be used with an acceptable accuracy when the mean velocity component is large compared to the velocity fluctuations. For a normal wire, the assumption of sensitivity only to the streamwise velocity fluctuations will become poorer as the fluctuations of the other component normal to the wire increase (by simple vector addition). Crossed-wire probes have a theoretical velocity vector wedge-angle limit defined by the normals to each wire. In practice, the allowable flow angle is much less than this owing to wakes which are shed from the prongs. The boundary layer turbulence encountered in the region of adverse pressure gradient is expected to increase to such an extent that these sources of error will become significant. One way around this problem is to fly the probe in the upstream direction at high speed while sampling on the basis of the probe position. The superimposed bias velocity will reduce the magnitude of the turbulent velocity fluctuations relative to the increased velocity seen by the probe so that accurate measurements are possible.

There is another, very distinct, advantage of flying the wire, i.e. measurements can be obtained on a very dense spatial grid. The time required to obtain converged data by repetitively scanning a dense grid can be more than an order of magnitude less than the time required to get the same data by traversing the probe to each point on the grid in succession and taking data with a stationary probe. At the low speeds of this experiment the sampling period must be as long as 100 seconds for adequate data convergence. In this case, the total time to obtain 30 points in a profile in the usual way with a stationary probe is of about 50 minutes duration. In regions where the turbulence intensity is not too high, the probe can be scanned up and down through the layer at

speeds that are quite high but not large enough relative to the mean flow to exceed the thresholds mentioned above. For example, with constant magnitude accelerations of alternating sign and a maximum speed limit of around 0.6 m/s, the oscillation frequency for traversing a distance of 32mm up and back down through a layer is about 4.5Hz. If samples are taken on the basis of the probe position and if 5,000 samples at each point are adequate for data convergence, then only 18 minutes is required to measure the entire profile compared to 50 minutes in the case of the stationary probe. However, a more significant benefit is that there is no time penalty for increasing the spatial density of the grid. For example, if samples are taken for each 0.025mm increment of the probe position, then the spatial density of the grid can be increased by a factor of more than 40 compared to the conventional method with a stationary probe. Also, spanwise derivatives and streamwise derivatives can be measured.

Calibration of crossed-wire probes requires a mechanism in addition to the probe traverse. For example, in dynamic calibration schemes the small perturbation sensitivity of the probe is determined directly by oscillating it back and forth continuously in a steady and uniform free-stream using a mechanical shaker. An alternative calibration scheme consists of imposing a number of flow angles on the probe by rotating it about an axis normal to the plane of the prongs. Intricate mechanisms are usually added to the traverse to perform this function. However, the same effect can be accomplished relative to the probe by moving it at high speed across a uniform free-stream. The advantage of a high speed 3D traverse is that either crossed-wire calibration scheme can be used without the need for additional hardware and without the need to handle probes.

Hot-wire probes must be calibrated frequently in a uniform stream. Using a conventional single-axis traversing system in the adverse pressure gradient experiments would require the removal and reinstallation of fragile and expensive probes from the measurement region for the purpose of calibration. This would be time consuming and risk probe breakage. With a high-speed traversing system this could be performed almost instantly as well as minimizing the chances of probe damage.

Since all the functions described above are under software control, the opportunity exists to create an intelligent system. For example, hot-wire calibration drift is a particularly common and frustrating phenomenon during the course of an experiment. At regular intervals, the probe could be rapidly moved to a reference point in the free-stream to check for drift and another calibration performed (automatically) if some tolerance level was exceeded.

4. Results to Date

4.1 Incoming laminar boundary layer

The boundary layer on the test plate has its origin upstream and, therefore,

it is influenced by the pressure gradients, wall curvature and lateral convergence within the contraction. Since the flow is accelerated by a contraction, the pressure gradients on the side walls are generally favourable. However, it can be shown that for a finite length contraction two regions of adverse pressure gradient exist on the walls in the vicinity of the entrance and the exit. Laminar boundary layers are especially sensitive to adverse pressure gradients and are prone to separation causing increased unsteadiness. Because of the low Reynolds number requirements of the current experiment, the quality of the incoming laminar boundary layer needs even more attention than usual.

Laminar boundary layer profiles were measured with a total pressure probe at a station 8.3cm downstream of the contraction exit for a number of free-stream velocities. The pressure was constant along the test section for these measurements. All the velocity profiles were found to be very near the Blasius profile. In particular the boundary layer corresponding to the lowest velocity of $U_o = 6.3$ m/s planned for the experiment has a shape factor $H=\frac{\delta^*}{\theta}=2.45$ which is close to that of the Blasius profile (H=2.59).

4.2 Selection of a transition device

The low Reynolds number requirements of the experiment dictates that measurements be obtained close to the boundary layer tripping device. The effect of a simple cylindrical wire has been the subject of many studies, see Schlichting (1979) p. 537 for a review. More recently there have been observations of spanwise irregularities in the boundary layers behind trip wires. Many workers have suggested that distributed three-dimensional roughness elements may be superior for transition purposes. However, the author is not aware of a systematic parametric study that offers a reproducible alternative to a trip wire. The observed irregularities have varying strengths depending on the facility. There is evidence to suggest (see Bradshaw 1965) that the observations are more closely associated with wind tunnel screens rather than with trip wires.

For the reasons outlined above, a simple wire was selected for boundary layer transition. The diameter and streamwise position for a number of wires were determined using the guidelines reported in Schlichting in conjunction with the laminar velocity profile measurements discussed earlier. Satisfactory results were obtained with 1.7mm and 2.0mm (diameter) wires when positioned near the contraction exit. However, when moved to a location 20cm downstream of the contraction, the 1.7mm wire failed to produce transition at all. Transition was intermittent with the 2.0mm wire at this location. These observations can be explained in terms of the adverse pressure gradient (not measured) near the exit of the contraction. Effective transition was obtained with a larger 2.4mm diameter wire at X=15cm. Measurements of C_f, momentum thickness and shape factor H indicated that a regular turbulent boundary layer is established behind the 2.4mm wire by $X \approx 25$cm corresponding to a momentum thickness $R_\theta \approx 450$.

4.3 Mean velocity profiles with the pressure gradient

The variation of C_p with streamwise distance is shown in figure 1(a). The streamwise spacing (5cm) of the measurements appears to be adequate since estimates of dC_p/dX obtained with four different numerical schemes are much the same as shown in figure 1(b). Mean velocity profiles were measured on the centerline (Z=0) with a 0.042 inch outside diameter total pressure probe which also functioned as a Preston tube for estimating the wall shear stress. The same probe was also used for the spanwise wall shear stress surveys. Mean pressures were determined over a 90 second period requiring about 45 minutes per profile and the data was acquired over a three day period. The probe was traversed under-computer control and once set running in the morning, the experiment proceeded without manual intervention throughout the day.

A number of interesting features can be determined from the data set. A list of quantities derived from the profile data is given in table 1 and some of these have been plotted in figures 2(a)-(f). For 35cm $< X <$ 55cm the layer thicknesses are approximately constant and the shape of the velocity profiles is similar as indicated by the shape factor. This suggests that the layer in this region is close to equilibrium. The profiles are shown in both wall- and outer-coordinates in both the region of the favorable and the adverse pressure gradients in figures 3(a)-(d). Estimates of the skin friction coefficient C_{fo} obtained from the Preston tube have been used to plot the profiles shown in wall-coordinates. The pressure gradients are well within the allowable limits suggested by Patel (1965). The deviations from the log law indicate that uncertainties of up to 10% in wall shear stress may have to be accepted.

4.4 Checks for two-dimensionality

The results of two spanwise C_f surveys are shown in figure 4(a). The location of the upstream survey corresponds to the region where the layer is in equilibrium. The survey spans approximately 40 boundary layer thicknesses and the variations are within $\pm$ 5% of the mean value. The downstream location in the region of adverse pressure gradient corresponds to $R_\theta \approx 1400$ which is within the capabilities of Spalart's simulations. The spanwise extent of the survey is about 20 layer thicknesses, and again the variations are within $\pm$ 5% of the mean value. The momentum balance shown in figure 4(b) is within 10%. The spanwise C_f measurements and the momentum balance indicate that the flow is acceptably two-dimensional.

5. Conclusions

The boundary layer in the remodelled Boundary Layer Wind Tunnel is closely related to the capabilities of Spalart's simulations. In particular, the layer appears to be close to equilibrium just before application of the adverse pressure gradient which is a suitable initial condition for a simulation. The pressure gradient parameter $\beta_x \approx 2$ at $R_\theta \approx 1650$ which is about the upper limit of the

numerical simulation capabilities. At this location, the distance downstream of the contraction is equal to the width of the test section. The spanwise variation of C_f is within $\pm$ 5% and the momentum balance is good.

The high-speed computer-controlled 3D traverse has unique capabilities that will allow hot-wire measurements with a high spatial density to be obtained very quickly. Accurate measurements can be obtained on the "fly" in regions of high turbulence intensity that would be otherwise be subject to gross uncertainties using stationary probes.

REFERENCES

BRADSHAW, P. 1965 The effect of wind tunnel screens on nominally two-dimensional boundary layers. *J. Fluid Mech.* **22**, 679.

INMAN, P.N. & BRADSHAW, P. 1981 Mixing length in low Reynolds number turbulent boundary layers. AIAA J. Vol. 19, No. 5, 653-655.

PATEL, V.C. 1965 Calibration of the Preston tube & limitations on its use in pressure gradients. *J. Fluid Mech.* **23**, 185-208.

SCHLICHTING, H. 1979 Boundary Layer Theory. 7^{th} ed. McGraw-Hill, New York.

SPALART, P.R. 1988 Direct simulation of a turbulent boundary layer up to R_θ=1410. *J. Fluid Mech.* **187**, 61-98.

X cm	C_p	δ_{99} mm	δ^* mm	θ mm	δ_3 mm	C_{f_c} x 10^3 Prest.	C_{f_c} x 10^3 Loglaw	H	β_z $\frac{\delta^*}{\tau_w}\frac{dP}{dx}$	R_θ	ΔU^+ max	C_{f_o} x 10^3 Using U_0
25	-0.20	8.50	1.56	1.00	0.75	5.75	5.68	1.555	-0.181	434.3	-	5.87
30	-0.60	10.27	1.60	1.06	0.82	5.85	5.75	1.501	-0.261	469.3	-	6.20
35	-0.10	11.03	1.67	1.13	0.88	5.71	5.65	1.477	-0.295	509.6	-	6.28
40	-0.17	11.69	1.68	1.14	0.90	5.62	5.60	1.465	-0.371	530.2	-	6.57
45	-0.24	12.07	1.66	1.13	0.90	5.52	5.59	1.467	-0.350	541.1	-	6.84
50	-0.31	12.92	1.73	1.19	0.94	5.36	5.50	1.457	-0.352	585.7	-	7.02
55	-0.38	13.02	1.75	1.20	0.95	5.26	5.47	1.453	-0.337	606.2	-	7.26
60	-0.41	13.27	1.78	1.24	0.98	5.28	5.41	1.440	-0.261	633.1	-	7.44
65	-0.40	14.35	2.05	1.41	1.11	4.89	5.16	1.450	0.198	717.4	0.140	6.84
70	-0.35	15.43	2.38	1.63	1.26	4.63	4.76	1.453	0.560	814.4	0.841	6.25
75	-0.27	17.23	2.81	1.91	1.44	4.29	4.42	1.474	0.748	925.6	1.550	5.45
80	-0.19	19.18	3.45	2.29	1.69	3.92	3.96	1.505	1.116	1074.0	2.650	4.67
85	-0.12	21.78	4.11	2.70	1.96	3.65	3.60	1.521	1.527	1229.0	3.640	4.09
90	-0.05	22.82	4.86	3.16	2.20	3.35	3.25	1.559	1.684	1392.0	4.930	3.52
95	-0.00	25.24	5.61	3.56	2.48	3.20	3.15	1.575	1.788	1531.0	5.150	3.20
100	0.06	27.33	6.35	3.98	2.73	3.08	2.89	1.595	2.008	1659.0	6.220	2.89
105	0.09	29.11	7.11	4.39	2.96	2.86	2.70	1.621	1.936	1800.0	7.080	2.60
110	0.12	31.61	7.83	4.80	3.21	2.85	2.56	1.630	1.731	1936.0	7.720	2.51
115	0.15	32.94	8.56	5.20	3.45	2.76	2.46	1.646	2.036	2061.0	8.340	2.35
120	0.19	34.69	9.28	5.59	3.67	2.69	2.36	1.661	2.392	2163.0	8.840	2.18
125	0.21	36.54	9.88	5.92	3.86	2.69	2.35	1.669	2.171	2262.0	8.820	2.13
130	0.22	39.17	10.54	6.32	4.13	2.68	2.30	1.666	1.790	2400.0	9.040	2.09
135	0.24	42.44	11.56	6.81	4.39	2.41	2.16	1.549	2.299	2553.0	9.860	1.83
140	0.26	44.31	12.18	7.15	4.61	2.41	2.10	1.703	1.909	2644.0	10.34	1.78

TABLE1. Streamwise Development of Mean Velocity Profiles with Pressure Gradient

NOTE:

1. **Reference inlet velocity $U_e \approx 6.5$ m/s at X=0cm.**
2. **Boundary layer trip wire is at X=15cm.**

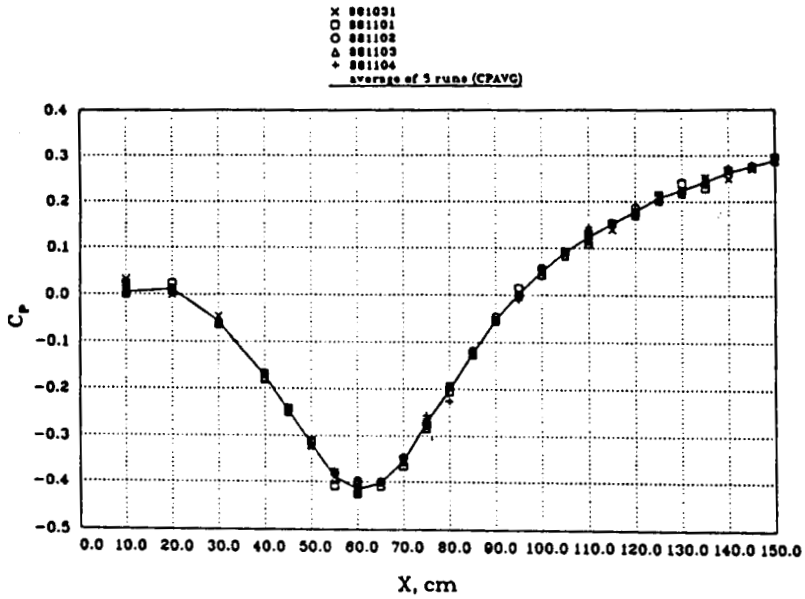

(a)

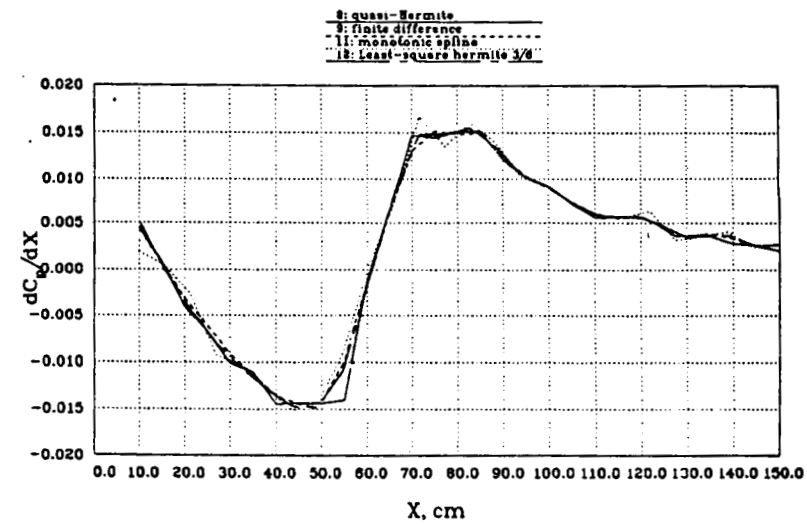

(b)

Figure 1(a) Variation of Pressure Coefficient C_p with streamwise distance.
(b) Estimates of dC_p/dX using four numerical schemes.

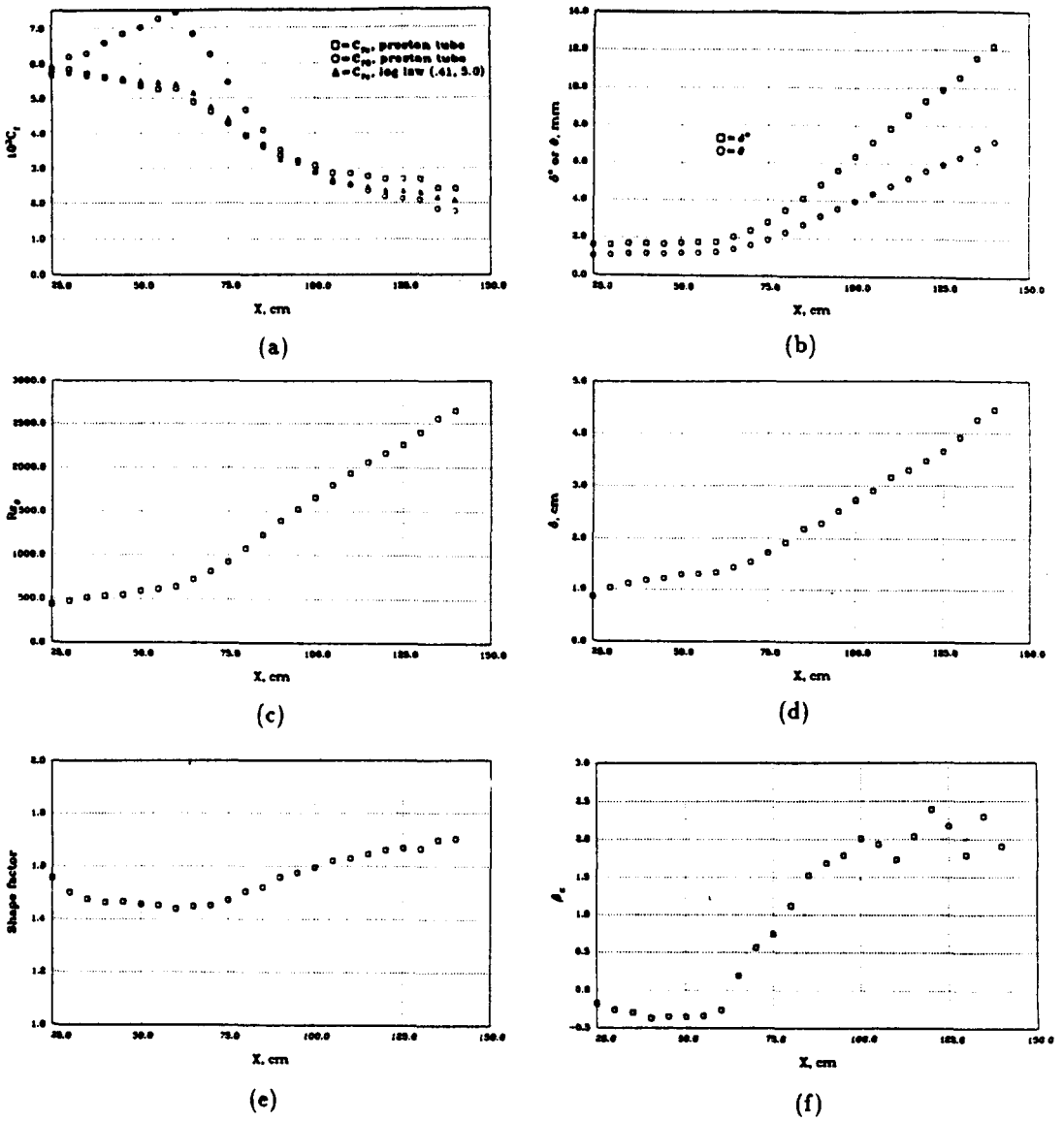

Figure 2. Variation of quantites derived from profile data with streamwise distance.
(a) Skin Friction Coefficient C_f (b) Displacement δ^* and momentum θ thicknesses
(c) Reynolds number based on momentum thickness R_θ (d) Boundary layer thickness δ
(e) Shape Factor H=$\frac{\delta^*}{\theta}$. (f) Pressure gradient parameter $\beta_z = \frac{\delta^*}{\tau_w}\frac{dP}{dz}$

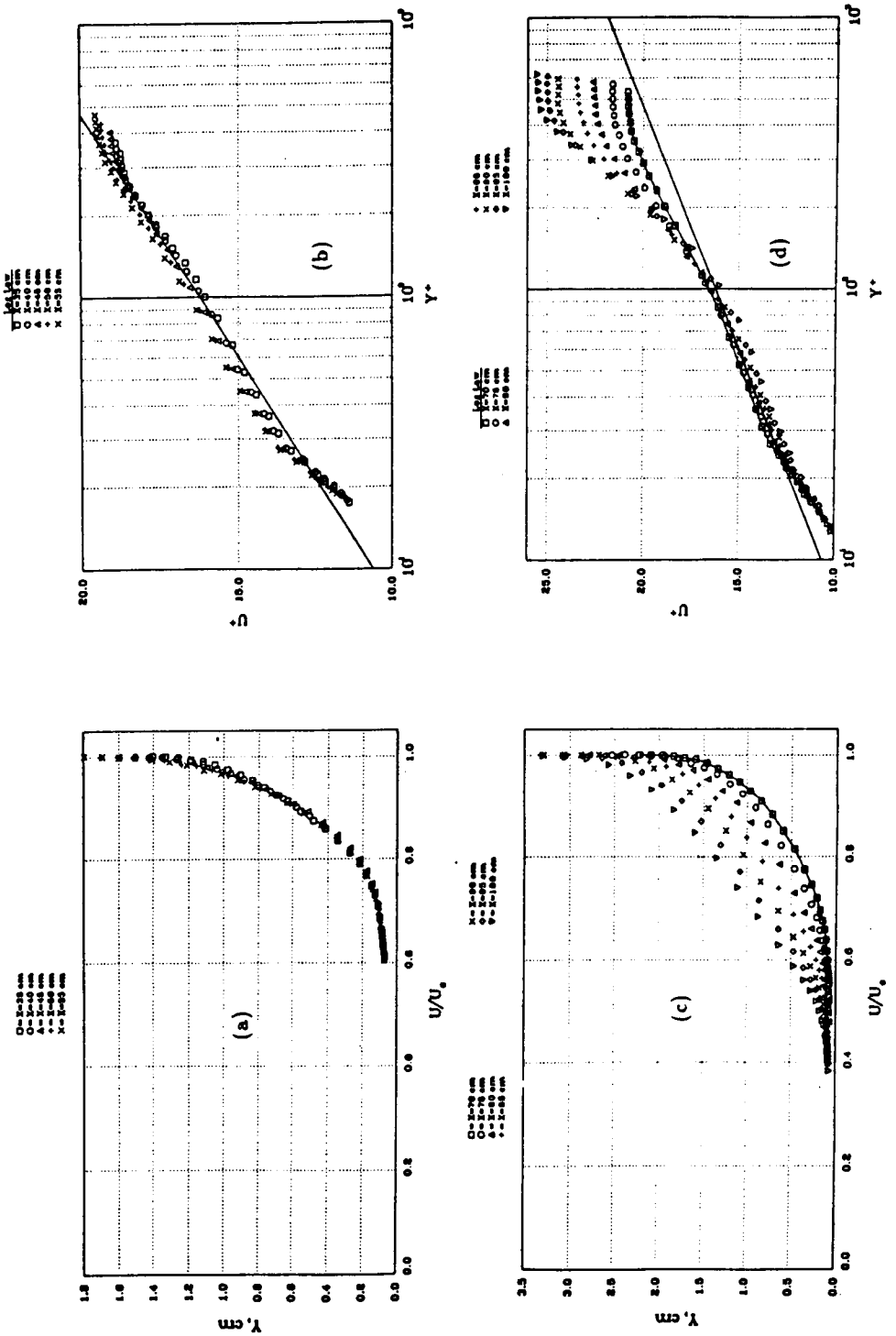

Figure 3. Mean velocity profiles.
(a) Region of favorable pressure gradient and (b) in wall coordinates.
(c) Region of adverse pressure gradient and (d) in wall coordinates.

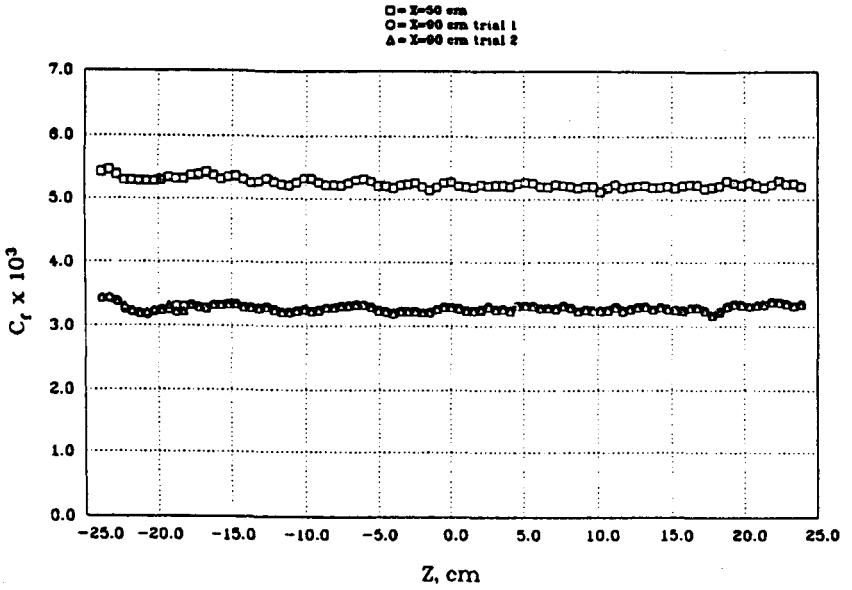

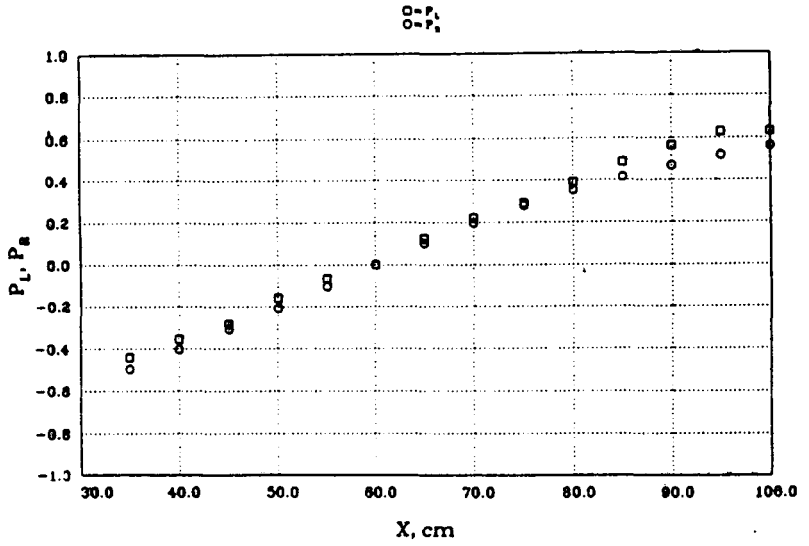

Figure 4(a) Spanwise variation of C_f at X=50cm and X=90cm.
(b) Momentum balance.